AIMS Mathematics, 11(1): 1–21.
DOI: 10.3934/math.2026001
Received: 26 September 2025
Revised: 15 December 2025
Accepted: 24 December 2025
Published: 04 January 2026

https://www.aimspress.com/journal/Math

Research article

A novel passivity-based energy-shaping tracking control strategy for networked underactuated Euler-Lagrange systems

Bin Zheng[1], **Runlong Peng**[2] **and Xuewei Ling**[3,*]

[1] School of Information Engineering, Fujian Business University, Fuzhou 350506, China
[2] Shanghai Institute of Applied Mathematics and Mechanics and Shanghai Key Laboratory of Mechanics in Energy Engineering, School of Mechanics and Engineering Science, Shanghai University, Shanghai 200072, China
[3] School of Mathematics and Computer Science, Quanzhou Normal University, Quanzhou 362000, China

* **Correspondence:** Email: lxw930628@163.com.

Abstract: This paper presents the innovative tracking control approach for networked underactuated Euler-Lagrange systems (NUELSs), which employs the energy-shaping method within the passivity-based control framework. By introducing adaptive control techniques and sliding mode variables, two passivity-based control schemes for NUELSs are developed to enhance the reliability and tracking performance. The proposed controllers achieve closed-loop stability and accurate trajectory tracking by shaping the system's energy and assigning appropriate damping, while maintaining robustness in the presence of communication delays. The rigorous Lyapunov-based analysis is conducted to prove that all internal signals remain bounded and that the tracking errors converge asymptotically to zero. Furthermore, numerical simulations further validate the effectiveness of the presented method.

Keywords: energy-shaping method; networked underactuated Euler-Lagrange systems (NUELSs); passivity-based control; sliding mode; communication delays
Mathematics Subject Classification: 34H05, 93A16, 93C10

1. Introduction

In recent years, networked underactuated Euler-Lagrange systems (NUELSs) have emerged as critical models in a wide range of advanced engineering applications, including cooperative robotic systems, spacecraft formation control, flexible manipulators, and underwater operating platforms, which have important research value and application prospects [1–5]. Since the dimensionality of the control inputs in the system is smaller than its number of degrees of freedom, and multiple

subsystems are interactively coupled through the network, the overall system is usually characterized by strong nonlinearity, complex coupling, and restricted state accessibility. Influenced by this structural constraint, NUELSs face significant challenges in realizing high-precision trajectory tracking control, especially when communication uncertainties may damage the closed-loop performance of the system, inducing system oscillations or even instability phenomena [6–8]. Such non-ideal network effects not only exacerbate the complexity of controller design, but also significantly affect the accuracy and convergence performance of the system trajectory tracking, which has become a key bottleneck in the current research of NUELSs [9–12].

It is well known that passivity-based control has become an important approach to solve the control problems of multi-agent systems (MASs) due to its ability to effectively preserve the natural energy structure of mechanical systems and its strong robustness, extensibility, and universality [13–16]. With this control framework, energy-shaping techniques are used to achieve closed-loop stability and performance tuning of the system by reconfiguring the potential and kinetic energy functions of the system to steer the system state towards the desired trajectory [17]. Extensive studies have been conducted on the design of passivity-based controllers using energy-shaping techniques for complex physical systems, yielding promising control performance in various applications [18–22]. Cruz-Zavala et al. proposed a derivation method for a novel family of distributed controllers, which can achieve finite-time leaderless and leader–follower consensus in networks of fully actuated Euler-Lagrange (EL) systems without requiring velocity measurements [18]. Sandoval et al. carried out the first systematic study on robotic joint position tracking by employing a localized potential shaping technique, which integrates energy shaping with total damping injection [20]. However, most existing studies have concentrated on either fully actuated EL systems. The application of passivity-based control methods to NUELSs remains relatively underexplored, which constitutes one of the primary motivations for this work.

lternatively, time delays is an inevitable phenomenon of networked control systems, arising from sensing, communication, computation, and actuation processes. Such delays, induced by packet loss, bandwidth limitations, and transmission latency, are often unavoidable in practice [23–25]. While small delays mainly affect transient responses, large or uncertain delays can substantially degrade coordination and even destabilize the system [26–28]. Considerable progress has been achieved in delay analysis and compensation for MASs, especially in consensus and synchronization of fully actuated EL dynamics. In contrast, research on NUELSs remains limited, where nonlinearities and strong couplings magnify the detrimental effects of communication delays. To bridge this gap, this paper develops the passivity-based energy-shaping control strategy for NUELSs with communication delays.

As a summary, this paper is oriented to the fundamental challenges such as nonlinear coupling and communication delays in the trajectory tracking control of NUELSs, and constructs a set of the energy shaping within the passivity-based control framework. By deeply reconstructing the energy structure of the system and combining the nonlinear control theory with the system dynamics characteristics, the method realizes the precise regulation of the trajectory error while ensuring the closed-loop stability. Compared with the existing work [8, 29–33], the main contributions include:

(1) A structurally explicit energy-shaping passivity-based control strategy is proposed, in which the potential and kinetic energy functions of NUELSs and the energy of the adaptive updating law are reconfigured and appropriate damping injection is introduced. This approach enables closed-loop

stability control and state regulation with underactuated and coupling constraints, thereby providing a unified modeling and design framework for trajectory tracking control of NUELSs.

(2) An adaptive regulation mechanism and sliding-mode-based auxiliary variables are incorporated to enhance the convergence performance of the energy-shaping controller under dynamic nonlinear conditions. This design significantly improves the system's regulation capability and robustness, while strengthening its applicability to practical networked scenarios.

(3) A comprehensive Lyapunov-based analysis is conducted to rigorously prove the uniform boundedness of all closed-loop state variables and the asymptotic convergence of the tracking errors. In addition, numerical simulations on the representative NUELSs are performed to demonstrate the proposed method's effectiveness in terms of tracking accuracy, response speed, and stability.

The organization of the paper is as follows. Section 2 formulates the dynamical model of NUELSs together with the essential preliminaries that underpin the subsequent analysis. Section 3 develops the passivity-based energy-shaping control strategy and rigorously addresses its applicability in the presence and absence of communication delays. Section 4 provides numerical simulations to demonstrate the effectiveness and robustness of the proposed methods. Finally, Section 5 concludes the main findings and discusses several promising directions for future research.

2. Preliminaries

2.1. Notation

To facilitate the subsequent analysis and controller design, the following symbols are defined. The set of real $b \times b$ matrices and the b-dimensional Euclidean space are denoted by $\mathbb{R}^{b\times b}$ and $\mathbb{R}^b$, the zero vector and the zero matrix are represented by $\mathbf{0}_b \in \mathbb{R}^b$ and $\mathbf{0}_{b\times b} \in \mathbb{R}^{b\times b}$, $\boldsymbol{I}_b \in \mathbb{R}^{b\times b}$ stands for the $b \times b$ identity matrix. The Kronecker product between matrices $\boldsymbol{X}$ and $\boldsymbol{Y}$ is symbolized by $\boldsymbol{X} \otimes \boldsymbol{Y}$, the symbols $\boldsymbol{X}^{-1}$, $\boldsymbol{X}^T$ designate the inverse and transpose of $\boldsymbol{X}$. The operator $diag\,(\cdot)$ produces a diagonal matrix with the given elements along the main diagonal, blockdiag$(\cdot)$ is the block-diagonal operator. $\|\cdot\|$ indicates the Euclidean norm when applied to vectors and the matrix-induced 2-norm when applied to matrices. The function $\kappa : [0,\infty) \to [0,\infty)$ is said to be of class-$\mathcal{K}$ if it is continuous, strictly increasing, and satisfies $\kappa(0) = 0$. For any vector $\boldsymbol{a} \in \mathbb{R}^b$, the gradient of a scalar function is defined as $\nabla_{\boldsymbol{a}} = \left(\frac{\partial}{\partial_{a_1}}, \cdots, \frac{\partial}{\partial_{a_b}}\right)^T \in \mathbb{R}^b$. Unless otherwise specified, all matrices are assumed to have compatible dimensions for the involved algebraic operations.

2.2. Graph theory

The communication topology among NUELSs is commonly described using graph-theoretic notions, and a brief overview of the relevant concepts is provided below. In general, the information exchange among $P(P \geq 2)$ underactuated EL systems is modeled by a weighted directed graph $\mathcal{D} = (\mathcal{U}, \zeta, \mathcal{B})$, which represents the communication topology. Here, $\mathcal{U} = \{1, 2, \cdots, P\}$ denotes the set of nodes corresponding to the agents, and $\zeta \subseteq \mathcal{U} \times \mathcal{U}$ refers to the set of directed edges. The adjacency matrix $\mathcal{B} = (a_{ij}) \in \mathbb{R}^{P\times P}$ quantifies the communication structure, where $a_{ij} = 1$ if there exists a directed edge from agent j to agent i, and $a_{ij} = 0$ otherwise. The Laplacian matrix is defined as $\boldsymbol{L} = (l_{ij}) \in \mathbb{R}^{P\times P}$, each diagonal element is given by $l_{ii} = \sum_{j=1}^{P} a_{ij}$, and each off-diagonal element is defined as $l_{ij} = -a_{ij}, i \neq j$. By construction, the row sums of L satisfy $\sum_{j=1}^{P} l_{ij} = 0$, ensuring the

conservation of flow in the network. A directed graph $\mathcal{D}$ is said to contain a directed spanning tree if there exists at least one root node that has a directed path to all other nodes in the network. To characterize the leader-follower communication topology, a diagonal matrix $\boldsymbol{L}_r = diag(\beta_1, \cdots \beta_P)$ is introduced, where $\beta_i > 0$, indicates that the i-th follower is directly influenced by the leader, and $\beta_i = 0$ otherwise. A comprehensive treatment of relevant graph-theoretic notions can be provided in [34].

2.3. Problem formulation

A network of P underactuated EL systems is considered, in which the dynamics of the i-th system is characterized by [8, 19]:

$$\begin{aligned} &\boldsymbol{M}_i(\boldsymbol{q}_i)\ddot{\boldsymbol{q}}_i + \boldsymbol{C}_i(\boldsymbol{q}_i, \dot{\boldsymbol{q}}_i)\dot{\boldsymbol{q}}_i + \boldsymbol{G}_i(\boldsymbol{q}_i) + \boldsymbol{F}_i(\boldsymbol{q}_i - \boldsymbol{x}_i) = \boldsymbol{0}_b; \\ &\boldsymbol{U}_i\ddot{\boldsymbol{x}}_i + \boldsymbol{F}_i(\boldsymbol{x}_i - \boldsymbol{q}_i) = \boldsymbol{\tau}_i, \end{aligned} \tag{2.1}$$

where $i = 1, 2, ..., P$, $\boldsymbol{q}_i \in \mathbb{R}^b$ and $\boldsymbol{x}_i \in \mathbb{R}^b$ denote the angular positions of the links and the motors (joints). The inertia matrix $\boldsymbol{M}_i(\boldsymbol{q}_i) \in \mathbb{R}^{b\times b}$ is assumed to be symmetric and positive definite. The term $\boldsymbol{C}_i(\boldsymbol{q}_i, \dot{\boldsymbol{q}}_i) \in \mathbb{R}^{b\times b}$ represents the Coriolis and centrifugal matrix, $\boldsymbol{G}_i(\boldsymbol{q}_i) \in \mathbb{R}^b$ stands for the gravitational torque vector. The motor inertia and joint stiffness matrices are denoted by $\boldsymbol{U}_i, \boldsymbol{F}_i \in \mathbb{R}^{b\times b}$, both of which are symmetric and positive definite. The control input is given by $\boldsymbol{\tau}_i \in \mathbb{R}^b$.

The NUELSs (2.1) are known to exhibit the following three structural properties [34].

Property 1. *It is assumed that the matrix $\dot{\boldsymbol{M}}_i(\boldsymbol{q}_i) - 2\boldsymbol{C}_i(\boldsymbol{q}_i, \dot{\boldsymbol{q}}_i)$ is skew-symmetric, i.e., for any vector $\boldsymbol{n} \in \mathbb{R}^b$, the following identity $\boldsymbol{n}^T \left[\dot{\boldsymbol{M}}_i(\boldsymbol{q}_i) - 2\boldsymbol{C}_i(\boldsymbol{q}_i, \dot{\boldsymbol{q}}_i)\right] \boldsymbol{n} = 0$ holds.*

Property 2. *The system dynamics can be linearly parameterized as $\boldsymbol{M}_i(\boldsymbol{q}_i)\boldsymbol{z}_1 + \boldsymbol{C}_i(\boldsymbol{q}_i, \dot{\boldsymbol{q}}_i)\boldsymbol{z}_2 + \boldsymbol{G}_i(\boldsymbol{q}_i) = \boldsymbol{Y}_i(\boldsymbol{q}_i, \dot{\boldsymbol{q}}_i, \boldsymbol{z}_1, \boldsymbol{z}_2)\boldsymbol{\eta}_i$, for any given vectors $\boldsymbol{z}_1, \boldsymbol{z}_2 \in \mathbb{R}^b$, where $\boldsymbol{Y}_i(\boldsymbol{q}_i, \dot{\boldsymbol{q}}_i, \boldsymbol{z}_1, \boldsymbol{z}_2)$ is the regressor matrix and $\boldsymbol{\eta}_i$ is the unknown parameter vector.*

Property 3. *The matrices and vectors associated with the NUELSs satisfy standard boundedness properties: $\chi_d \boldsymbol{I}_b \leq \boldsymbol{M}_i(\boldsymbol{q}_i) \leq \chi_D \boldsymbol{I}_b$, $\left\|\boldsymbol{C}_i(\boldsymbol{q}_i, \dot{\boldsymbol{q}}_i)\right\| \leq \chi_e \left\|\dot{\boldsymbol{q}}_i\right\|$ and $\left\|\boldsymbol{G}_i(\boldsymbol{q}_i)\right\| \leq \chi_f$, where χ_d, χ_D, χ_e and χ_f are positive constants.*

The passivity-based energy-shaping control strategy is proposed to address the tracking problems for NUELSs. The suggested approach ensures that all agents accurately track a common reference trajectory while reaching consensus in their states. To support the subsequent theoretical development, the tracking control problem is formally defined as follows:

Definition 1. *For the NUELSs (2.1), the tracking control problems are considered to be solved if there exists the control input $\boldsymbol{\tau}_i$ such that the position trajectory asymptotically converge to a common time-varying reference trajectory $\boldsymbol{q}_d(t) \in \mathbb{R}^b$, provided that at least one agent has direct access to the reference signal. That is, for every agent $i \in [1, P]$, the following conditions hold*

$$\lim_{t\to\infty} \left\|\hat{\boldsymbol{q}}_i\right\| = \left\|\boldsymbol{q}_i(t) - \boldsymbol{q}_d(t)\right\| = 0, \left\|\dot{\hat{\boldsymbol{q}}}_i\right\| = \lim_{t\to\infty} \left\|\dot{\boldsymbol{q}}_i(t) - \dot{\boldsymbol{q}}_d(t)\right\| = 0. \tag{2.2}$$

Remark 1. *The intrinsic difficulty in controlling NUELSs arises from the structural mismatch between the number of control inputs and the system's degrees of freedom. This mismatch implies that some degrees of freedom cannot be actuated independently, and the controller must therefore rely on the*

nonlinear and configuration-dependent internal couplings of the system dynamics to achieve regulation or tracking [7–9]. Such couplings restrict the range of admissible control actions and substantially increase the complexity of Lyapunov-based stability analysis. Moreover, the lack of full actuation prevents arbitrary assignment of the closed-loop dynamics or direct shaping of the total energy, which leads to inherent performance limitations that do not occur in fully actuated systems [9–12]. These challenges fundamentally distinguish NUELSs from their fully actuated counterparts and motivate the passivity-based design framework developed in this work.

Remark 2. *Definition 1 extends the conventional time-invariant formulation to the tracking control problems of NUELSs (2.1) in the leader–follower network framework. In contrast to prior works [8, 17, 31, 32] that predominantly address convergence to static equilibria, the present setting necessitates asymptotic tracking of time-varying consensus trajectories. Moreover, the intrinsic nonlinearities and strong interconnections among NUELSs significantly increase the complexity of the time-varying problem compared with its time-invariant counterpart.*

3. Main results

3.1. Passivity-based tracking control without communication delays

This section is devoted to formulating the passivity-based control strategy for NUELSs (2.1) by applying the energy-shaping method without communication delays. For the purpose of theoretical development, the following assumptions and lemmas are presented.

Assumption 1. *The directed graph $\mathcal{D}$ associated with the NUELSs (2.1) is assumed to contain a directed spanning tree.*

Assumption 2. *It is assumed that the position information of the virtual leader is available to at least one of the P nonidentical follower systems.*

Lemma 1. *[30] If Assumption 1 is satisfied, then the matrix $\boldsymbol{L}$ has positive real parts for all eigenvalues. If exists matrix $\boldsymbol{A}$ is a positive definite, $\boldsymbol{B}=\boldsymbol{A}\boldsymbol{L}+\boldsymbol{L}^T\boldsymbol{A}$ is a positive definite matrix.*

Lemma 2. *[35] For the system*

$$\dot{\boldsymbol{y}} = f(t, \boldsymbol{y}) \tag{3.1}$$

with $f : [0,\infty) \times \mathbb{R}^b \to \mathbb{R}^b$ being piecewise continuous in t and locally Lipschitz in $\boldsymbol{y}$, let $Z : [0,\infty) \times \mathbb{R}^b \to \mathbb{R}$ be a continuously differentiable function such that

$$\kappa_1(\|\boldsymbol{y}\|) \le Z(t, \boldsymbol{y}) \le \kappa_2(\|\boldsymbol{y}\|), \tag{3.2}$$

$$\frac{\partial Z}{\partial t} + \frac{\partial Z}{\partial \boldsymbol{y}} f(t, \boldsymbol{y}) \le -\vartheta(\boldsymbol{y}), \forall \|y\| \ge \alpha > 0, \tag{3.3}$$

$\forall t \ge 0$ and $\forall \boldsymbol{y} \in \mathbb{R}^b$, where κ_1 and κ_2 are class-$\mathcal{K}$ functions and $\vartheta(\boldsymbol{y})$ is continuous positive-definite function. Then there exists $\bar{T} \ge 0$ (dependent on $\boldsymbol{y}(0)$ and α) such that the solution of Eq (3.1) satisfies

$$\|\boldsymbol{y}(t)\| \le \kappa_1^{-1}(\kappa_2(\alpha)), \forall t \ge \bar{T}. \tag{3.4}$$

To facilitate the the design of controller, the reference velocity vector $\dot{\boldsymbol{s}}_i \in \mathbb{R}^b$ is defined as

$$\dot{\boldsymbol{s}}_i = -k\sum_{j=1}^{P} a_{ij}\left(\hat{\boldsymbol{q}}_i - \hat{\boldsymbol{q}}_j\right) - k\beta_i\hat{\boldsymbol{q}}_i + \dot{\boldsymbol{q}}_d, \tag{3.5}$$

where k denotes the coupling strength among the agents. Thus, the sliding mode vector $\dot{\boldsymbol{\psi}}_i \in \mathbb{R}^b$ is formulated as

$$\dot{\boldsymbol{\psi}}_i = \dot{\boldsymbol{q}}_i - \dot{\boldsymbol{s}}_i. \tag{3.6}$$

Next, by defining two intermediate variables $\boldsymbol{e}_i \in \mathbb{R}^b$ and $\boldsymbol{r}_i \in \mathbb{R}^b$ as follows

$$\boldsymbol{e}_i = \boldsymbol{x}_i - \boldsymbol{r}_i, \tag{3.7}$$

and

$$\boldsymbol{r}_i = \boldsymbol{q}_i + \boldsymbol{F}_i^{-1}\boldsymbol{Y}_i\check{\boldsymbol{\eta}}_i - \boldsymbol{\psi}_i, \tag{3.8}$$

where $\check{\boldsymbol{\eta}}_i$ is the estimate of $\boldsymbol{\eta}_i$.

Then the corresponding updating law can be chosen as

$$\dot{\check{\boldsymbol{\eta}}}_i = -\boldsymbol{\delta}_i\boldsymbol{Y}_i^T\left(\boldsymbol{q}_i, \dot{\boldsymbol{q}}_i, \dot{\boldsymbol{s}}_i, \ddot{\boldsymbol{s}}_i\right)\dot{\boldsymbol{\psi}}_i, \tag{3.9}$$

where $\boldsymbol{\delta}_i$ represents a symmetric and positive definite matrix.

Therefore, the passivity-based control input for the i-th underactuated EL system is given by

$$\boldsymbol{\tau}_i = \boldsymbol{F}_i\left(\boldsymbol{x}_i - \boldsymbol{q}_i\right) - \boldsymbol{Q}_i\left(\boldsymbol{e}_i - \boldsymbol{\varepsilon}_i\right) - \boldsymbol{F}_i\left(\boldsymbol{e}_i - \boldsymbol{\psi}_i\right) + \boldsymbol{U}\ddot{\boldsymbol{r}}_i, \tag{3.10}$$

where $\boldsymbol{\varepsilon}_i \in \mathbb{R}^b$ stands for the generalized coordinate of the controller, and the matrix $\boldsymbol{Q}_i \in \mathbb{R}^{b\times b}$ refers to the springs stiffness coefficients.

The following system result from substituting Eqs (3.6)–(3.8) and (3.10) into system (2.1).

$$\begin{aligned} &\boldsymbol{M}_i\left(\boldsymbol{q}_i\right)\left(\ddot{\boldsymbol{\psi}}_i + \ddot{\boldsymbol{s}}_i\right) + \boldsymbol{C}_i\left(\boldsymbol{q}_i, \dot{\boldsymbol{q}}_i\right)\left(\dot{\boldsymbol{\psi}}_i + \dot{\boldsymbol{s}}_i\right) + \boldsymbol{G}_i\left(\boldsymbol{q}_i\right) - \boldsymbol{Y}_i\check{\boldsymbol{\eta}}_i + \boldsymbol{F}_i\left(\boldsymbol{\psi}_i - \boldsymbol{e}_i\right) = \boldsymbol{0}_b; \\ &\boldsymbol{U}_i\ddot{\boldsymbol{e}}_i + \boldsymbol{F}_i\left(\boldsymbol{e}_i - \boldsymbol{\psi}_i\right) = -\boldsymbol{Q}_i\left(\boldsymbol{e}_i - \boldsymbol{\varepsilon}_i\right). \end{aligned} \tag{3.11}$$

From Property 2, it can be derived that

$$\boldsymbol{M}_i\left(\boldsymbol{q}_i\right)\ddot{\boldsymbol{s}}_i + \boldsymbol{C}_i\left(\boldsymbol{q}_i, \dot{\boldsymbol{q}}_i\right)\dot{\boldsymbol{s}}_i + \boldsymbol{G}_i\left(\boldsymbol{q}_i\right) = \boldsymbol{Y}_i\left(\boldsymbol{q}_i, \dot{\boldsymbol{q}}_i, \dot{\boldsymbol{s}}_i, \ddot{\boldsymbol{s}}_i\right)\boldsymbol{\eta}_i. \tag{3.12}$$

Finally, the system (2.1) can be further rewritten in the form of the following closed-loop controlled systems

$$\begin{aligned} &\boldsymbol{M}_i\left(\boldsymbol{q}_i\right)\ddot{\boldsymbol{\psi}}_i + \boldsymbol{C}_i\left(\boldsymbol{q}_i, \dot{\boldsymbol{q}}_i\right)\dot{\boldsymbol{\psi}}_i + \boldsymbol{Y}_i\hat{\boldsymbol{\eta}}_i + \boldsymbol{F}_i\left(\boldsymbol{\psi}_i - \boldsymbol{e}_i\right) = \boldsymbol{0}_b; \\ &\boldsymbol{U}_i\ddot{\boldsymbol{e}}_i + \boldsymbol{F}_i\left(\boldsymbol{e}_i - \boldsymbol{\psi}_i\right) = -\boldsymbol{Q}_i\left(\boldsymbol{e}_i - \boldsymbol{\varepsilon}_i\right), \end{aligned} \tag{3.13}$$

where the estimated error $\hat{\boldsymbol{\eta}}_i = \boldsymbol{\eta}_i - \check{\boldsymbol{\eta}}_i$.

To proceed, the following expressions present the controller dynamics and its total energy function, derived from the equations of motion of the networked EL systems

$$\boldsymbol{M}_a\ddot{\boldsymbol{\varepsilon}} + \boldsymbol{H}\dot{\boldsymbol{\varepsilon}} + \nabla_{\varepsilon^c}\boldsymbol{N}\left(\boldsymbol{e}, \boldsymbol{\varepsilon}\right) = \boldsymbol{0}_{Pb}, \tag{3.14}$$

and

$$^{c}\boldsymbol{T}(\boldsymbol{e},\boldsymbol{\varepsilon},\dot{\boldsymbol{\varepsilon}}) = {}^{c}\boldsymbol{W}(\boldsymbol{\varepsilon},\dot{\boldsymbol{\varepsilon}}) + {}^{c}\boldsymbol{N}(\boldsymbol{e},\boldsymbol{\varepsilon}), \tag{3.15}$$

where $\boldsymbol{e} = \left[\boldsymbol{e}_1^T, \cdots, \boldsymbol{e}_P^T\right]^T \in \mathbb{R}^{Pb}$, $\boldsymbol{\varepsilon} = \left[\boldsymbol{\varepsilon}_1^T, \cdots, \boldsymbol{\varepsilon}_P^T\right]^T \in \mathbb{R}^{Pb}$ is the generalized coordinate, the matrix $\boldsymbol{M}_a \in \mathbb{R}^{Pb\times Pb}$ denotes positive semidefinite inertia, $\boldsymbol{H} = diag(h_i\boldsymbol{I}_n) \in \mathbb{R}^{Pb\times Pb}$ represents the damping matrix with $h_i > 0$. The kinetic energy of the controller is defined as $^{c}\boldsymbol{W}(\boldsymbol{\varepsilon},\dot{\boldsymbol{\varepsilon}}) = \frac{1}{2}\dot{\boldsymbol{\varepsilon}}^T\boldsymbol{M}_a\dot{\boldsymbol{\varepsilon}}$, and the corresponding potential energy with respect to the actuated component of NUELSs is given by $^{c}\boldsymbol{N}(\boldsymbol{e},\boldsymbol{\varepsilon}) = \frac{1}{2}(\boldsymbol{e}-\boldsymbol{\varepsilon})^T\boldsymbol{Q}(\boldsymbol{e}-\boldsymbol{\varepsilon})$.

Prior works [17, 18] show that the inertia matrix of the controller dynamics has negligible impact on the stability mechanism. Therefore, by setting $\boldsymbol{M}_a = \boldsymbol{I}_{Pb}$ and omitting the gravity terms throughout the analysis, the controller dynamics of the i-th EL system is given by

$$\ddot{\boldsymbol{\varepsilon}}_i = -h_i\dot{\boldsymbol{\varepsilon}}_i - \boldsymbol{Q}_i(\boldsymbol{\varepsilon}_i - \boldsymbol{e}_i). \tag{3.16}$$

For the closed-loop system described by Eq (3.13), the corresponding energy functions are derived as

$$^{s}\boldsymbol{T}\left(\boldsymbol{\psi},\boldsymbol{e},\dot{\boldsymbol{\psi}},\dot{\boldsymbol{e}}\right) = {}^{s}\boldsymbol{W}\left(\boldsymbol{\psi},\boldsymbol{e},\dot{\boldsymbol{\psi}},\dot{\boldsymbol{e}}\right) + {}^{s}\boldsymbol{N}(\boldsymbol{\psi},\boldsymbol{e}), \tag{3.17}$$

where $^{s}\boldsymbol{W}\left(\boldsymbol{\psi},\boldsymbol{e},\dot{\boldsymbol{\psi}},\dot{\boldsymbol{e}}\right) = \sum_{i=1}^{P} {}^{s}\boldsymbol{W}_i\left(\boldsymbol{\psi}_i,\boldsymbol{e}_i,\dot{\boldsymbol{\psi}}_i,\dot{\boldsymbol{e}}_i\right)$, with the kinetic energy function is defined as

$$^{s}\boldsymbol{W}_i\left(\boldsymbol{\psi}_i,\boldsymbol{e}_i,\dot{\boldsymbol{\psi}}_i,\dot{\boldsymbol{e}}_i\right) = \frac{1}{2}\left(\dot{\boldsymbol{\psi}}_i^T\boldsymbol{M}_i(\boldsymbol{q}_i)\dot{\boldsymbol{\psi}}_i + \dot{\boldsymbol{e}}_i^T\boldsymbol{U}_i\dot{\boldsymbol{e}}_i\right), \tag{3.18}$$

and $^{s}\boldsymbol{N}(\boldsymbol{\psi},\boldsymbol{e}) = \sum_{i=1}^{P} {}^{s}\boldsymbol{N}_i(\boldsymbol{\psi}_i,\boldsymbol{e}_i)$, with the potential energy function is express as

$$^{s}\boldsymbol{N}_i(\boldsymbol{\psi}_i,\boldsymbol{e}_i) = \frac{1}{2}(\boldsymbol{\psi}_i - \boldsymbol{e}_i)^T\boldsymbol{F}_i(\boldsymbol{\psi}_i - \boldsymbol{e}_i). \tag{3.19}$$

Remark 3. *The control input (3.10) within the passivity-based energy-shaping framework admits a clear physical interpretation and can be decomposed into four distinct components. Specifically, the first component $\boldsymbol{F}_i(\boldsymbol{x}_i - \boldsymbol{q}_i)$ is a linear feedback term with respect to the state of the NUELSs (2.1), the second component $\boldsymbol{Q}_i(\boldsymbol{e}_i - \boldsymbol{\varepsilon}_i)$ is a feedback term related to the intermediate variable* (3.7) *and the controller dynamics* (3.16)*, the third component $\boldsymbol{F}_i(\boldsymbol{e}_i - \boldsymbol{\psi}_i)$ combines a linear feedback term based on the intermediate variable* (3.7) *and the sliding mode vector* (3.6)*, and the fourth component $\boldsymbol{U}\ddot{\boldsymbol{r}}_i$ is a compensation term incorporating the system structure along with the adaptive updating law* (3.9)*. Moreover, the design of these four terms is fundamentally grounded in the controller dynamics and the associated sliding mode vector, and the tracking control strategy is ensured to be realized using the passivity-based energy-shaping control approach and the adaptive gain technique.*

Theorem 1. *For the NUELSs (2.1) under Assumptions 1 and 2, the proposed passivity-based control protocol (3.10) with the updating law (3.9) can solve the tracking problem in the sense of Definition 1.*

Proof. The total energy function associated with the closed-loop controlled system can be formulated

as the following Lyapunov function

$$\begin{aligned} V_1 =& {}^{s}I + {}^{c}I + {}^{r}I \\ =& \frac{1}{2}\begin{bmatrix} \dot{\boldsymbol{\psi}}^T & \dot{\boldsymbol{e}}^T & \dot{\boldsymbol{\varepsilon}}^T \end{bmatrix} \begin{bmatrix} \boldsymbol{M}(\boldsymbol{q}) & \mathbf{0}_{Pb\times Pb} & \mathbf{0}_{Pb\times Pb} \\ \mathbf{0}_{Pb\times Pb} & \boldsymbol{U} & \mathbf{0}_{Pb\times Pb} \\ \mathbf{0}_{Pb\times Pb} & \mathbf{0}_{Pb\times Pb} & \boldsymbol{M}_a \end{bmatrix} \begin{bmatrix} \dot{\boldsymbol{\psi}} \\ \dot{\boldsymbol{e}} \\ \dot{\boldsymbol{\varepsilon}} \end{bmatrix} \\ & + \frac{1}{2}\begin{bmatrix} \boldsymbol{\psi}^T & \boldsymbol{e}^T & \boldsymbol{\varepsilon}^T \end{bmatrix} \begin{bmatrix} \boldsymbol{F} & -\boldsymbol{F} & \mathbf{0}_{Pb\times Pb} \\ -\boldsymbol{F} & \boldsymbol{F}+\boldsymbol{Q} & -\boldsymbol{Q} \\ \mathbf{0}_{Pb\times Pb} & -\boldsymbol{Q} & \boldsymbol{Q} \end{bmatrix} \begin{bmatrix} \boldsymbol{\psi} \\ \boldsymbol{e} \\ \boldsymbol{\varepsilon} \end{bmatrix} \\ & + \frac{1}{2}\hat{\boldsymbol{\eta}}^T \boldsymbol{\delta}^{-1}\hat{\boldsymbol{\eta}} \\ =& \frac{1}{2}\dot{\boldsymbol{o}}^T \bar{\boldsymbol{A}}\dot{\boldsymbol{o}} + \frac{1}{2}\boldsymbol{o}^T \bar{\boldsymbol{B}}\boldsymbol{o} + \frac{1}{2}\hat{\boldsymbol{\eta}}^T \boldsymbol{\delta}^{-1}\hat{\boldsymbol{\eta}}, \end{aligned} \tag{3.20}$$

where $\boldsymbol{\psi} = \left[\boldsymbol{\psi}_1^T, \cdots, \boldsymbol{\psi}_P^T\right]^T$, $\hat{\boldsymbol{\eta}} = \left[\hat{\boldsymbol{\eta}}_1^T, \cdots, \hat{\boldsymbol{\eta}}_P^T\right]^T$, $\boldsymbol{M}(q) = blockdiag\left(\boldsymbol{M}_i(q_i)\right)$, $\boldsymbol{U} = blockdiag\left(\boldsymbol{U}_i\right)$, $\boldsymbol{\delta} = blockdiag\left(\boldsymbol{\delta}_i\right)$, $\boldsymbol{F} = blockdiag\left(\boldsymbol{F}_i\right)$, $\boldsymbol{Q} = blockdiag\left(\boldsymbol{Q}_i\right)$, $\boldsymbol{o} = [\ \boldsymbol{\psi}^T \quad \boldsymbol{e}^T \quad \boldsymbol{\varepsilon}^T\ ]^T$, $\bar{\boldsymbol{A}} = diag\left(\boldsymbol{M}(\boldsymbol{q}), \boldsymbol{U}, \boldsymbol{M}_a\right)$ and

$$\bar{\boldsymbol{B}} = \begin{bmatrix} \boldsymbol{F} & -\boldsymbol{F} & \mathbf{0}_{Pb\times Pb} \\ -\boldsymbol{F} & \boldsymbol{F}+\boldsymbol{Q} & -\boldsymbol{Q} \\ \mathbf{0}_{Pb\times Pb} & -\boldsymbol{Q} & \boldsymbol{Q} \end{bmatrix}.$$

By applying Properties 1 and 3, and utilizing Eqs (3.13) and (3.16) to Eq (3.20), the time derivative of Eq (3.20) can be obtained as

$$\begin{aligned} \dot{V}_1 =& \dot{\boldsymbol{\psi}}^T \boldsymbol{M}(\boldsymbol{q})\ddot{\boldsymbol{\psi}} + \frac{1}{2}\dot{\boldsymbol{\psi}}^T \dot{\boldsymbol{M}}(\boldsymbol{q})\dot{\boldsymbol{\psi}} + \dot{\boldsymbol{e}}^T \boldsymbol{U}\ddot{\boldsymbol{e}} + \dot{\boldsymbol{\varepsilon}}^T \ddot{\boldsymbol{\varepsilon}} \\ & + \left(\dot{\boldsymbol{\psi}} - \dot{\boldsymbol{e}}\right)^T \boldsymbol{F}(\boldsymbol{\psi} - \boldsymbol{e}) + (\dot{\boldsymbol{e}} - \dot{\boldsymbol{\varepsilon}})^T \boldsymbol{Q}(\boldsymbol{e} - \boldsymbol{\varepsilon}) + \hat{\boldsymbol{\eta}}^T \boldsymbol{\delta}^{-1}\dot{\hat{\boldsymbol{\eta}}} \\ =& -\dot{\boldsymbol{\psi}}^T \boldsymbol{Y}\hat{\boldsymbol{\eta}} - \dot{\boldsymbol{e}}^T \boldsymbol{Q}(\boldsymbol{e} - \boldsymbol{\varepsilon}) - \dot{\boldsymbol{\varepsilon}}^T \boldsymbol{H}\dot{\boldsymbol{\varepsilon}} - \dot{\boldsymbol{\varepsilon}}^T \boldsymbol{Q}(\boldsymbol{\varepsilon} - \boldsymbol{e}) \\ & + (\dot{\boldsymbol{e}} - \dot{\boldsymbol{\varepsilon}})^T \boldsymbol{Q}(\boldsymbol{e} - \boldsymbol{\varepsilon}) - \hat{\boldsymbol{\eta}}^T \boldsymbol{\delta}^{-1}\dot{\hat{\boldsymbol{\eta}}} \\ =& -\dot{\boldsymbol{\psi}}^T \boldsymbol{Y}\hat{\boldsymbol{\eta}} - \dot{\boldsymbol{\varepsilon}}^T \boldsymbol{H}\dot{\boldsymbol{\varepsilon}} + \hat{\boldsymbol{\eta}}^T \boldsymbol{Y}^T \dot{\boldsymbol{\psi}} \\ =& -\dot{\boldsymbol{\varepsilon}}^T \boldsymbol{H}\dot{\boldsymbol{\varepsilon}} \leq 0. \end{aligned} \tag{3.21}$$

It follows from Eq (3.21) that V_1 is a non-increasing and bounded function. Moreover, by employing the controller dynamics in Eq (3.16), one can deduce that $\ddot{\boldsymbol{\varepsilon}}_i$ is bounded, which implies that $\dot{V}_1$ is also bounded. Therefore, by invoking Barbalat's lemma [35], it can be concluded that $\lim_{t\to\infty} \dot{V}_1 = 0$, which further implies that $\lim_{t\to\infty} \dot{\boldsymbol{\varepsilon}}_i = \mathbf{0}_b$.

Thus, the application of the controller dynamics in Eq (3.16) yields:

$$\frac{d}{dt}\ddot{\boldsymbol{\varepsilon}}_i = -h_i\ddot{\boldsymbol{\varepsilon}}_i - \boldsymbol{Q}_i\left(\dot{\boldsymbol{\varepsilon}}_i - \dot{\boldsymbol{e}}_i\right). \tag{3.22}$$

Furthermore, it follows that $\dot{\boldsymbol{\varepsilon}}_i$, $\ddot{\boldsymbol{\varepsilon}}_i$, and $\dot{\boldsymbol{e}}_i$ are all bounded, which implies that $\frac{d}{dt}\ddot{\boldsymbol{\varepsilon}}_i$ is also bounded. Hence, $\ddot{\boldsymbol{\varepsilon}}_i$ is uniformly continuous. According to Barbalat's Lemma, it has $\lim_{t\to\infty} \ddot{\boldsymbol{\varepsilon}}_i = \mathbf{0}_b$. By applying

the Barbalat's Lemma again, it follows that $\lim_{t\to\infty} \frac{d}{dt}\ddot{\boldsymbol{\varepsilon}}_i = \mathbf{0}_b$. Moreover, from Eq (3.22), it concludes that $\lim_{t\to\infty} \dot{\boldsymbol{e}}_i = \mathbf{0}_b$.

Then, applying the closed-loop system (3.13) yields

$$\frac{d}{dt}\ddot{\boldsymbol{e}}_i + \boldsymbol{U}_i^{-1}\boldsymbol{F}_i\left(\dot{\boldsymbol{e}}_i - \dot{\boldsymbol{\psi}}_i\right) = -\boldsymbol{U}_i^{-1}\boldsymbol{Q}_i\left(\dot{\boldsymbol{e}}_i - \dot{\boldsymbol{\varepsilon}}_i\right). \tag{3.23}$$

By employing the same approach, the boundedness of $\dot{\boldsymbol{e}}_i$, $\ddot{\boldsymbol{e}}_i$, $\dot{\boldsymbol{\psi}}_i$, and $\dot{\boldsymbol{\varepsilon}}_i$ ensures that $\frac{d}{dt}\ddot{\boldsymbol{e}}_i$ remains bounded, indicating that $\ddot{\boldsymbol{e}}_i$ is uniformly continuous. As a result, Barbalat's Lemma yields $\lim_{t\to\infty} \ddot{\boldsymbol{e}}_i = \mathbf{0}_b$, which further leads to $\lim_{t\to\infty} \dot{\boldsymbol{\psi}}_i = \mathbf{0}_b$ by Eq (3.23).

Taking a simple deformation of Eqs (3.5) and (3.6), the resulting expressions can be rewritten in vector form

$$\dot{\hat{\boldsymbol{q}}} = -\left(\boldsymbol{W} \otimes \boldsymbol{I}_b\right)\hat{\boldsymbol{q}} + \dot{\boldsymbol{\psi}}, \tag{3.24}$$

where

$$\boldsymbol{W}{=}k\left(\boldsymbol{L} + \boldsymbol{L}_r\right), \quad \hat{\boldsymbol{q}} = \left[\hat{\boldsymbol{q}}_1^T, \cdots, \hat{\boldsymbol{q}}_P^T\right]^T, \quad \dot{\boldsymbol{\psi}} = \left[\dot{\boldsymbol{\psi}}_1^T, \cdots, \dot{\boldsymbol{\psi}}_P^T\right]^T.$$

From Assumption 1 and Lemma 1, one can conclude that $-\boldsymbol{W}$ is Hurwitz. Consequently, the Lyapunov function is constructed as

$$\bar{V}_1 = \hat{\boldsymbol{q}}^T\left(\boldsymbol{A}_1 \otimes \boldsymbol{I}_b\right)\hat{\boldsymbol{q}}, \tag{3.25}$$

where $\boldsymbol{A}_1$ is a positive definite matrix. Hence, the following result can be easily established

$$\lambda_{\min}\left(\boldsymbol{A}_1\right)\|\hat{\boldsymbol{q}}\|^2 \le \bar{V}_1 \le \lambda_{\max}\left(\boldsymbol{A}_1\right)\|\hat{\boldsymbol{q}}\|^2, \tag{3.26}$$

where $\lambda_{\min}\left(\boldsymbol{A}_1\right)$ and $\lambda_{\max}\left(\boldsymbol{A}_1\right)$ are the minimum and maximum eigenvalues of matrix $\boldsymbol{A}_1$, the time derivative of $\bar{V}_1$ is given by

$$\begin{aligned}\dot{\bar{V}}_1 =& \hat{\boldsymbol{q}}^T\left(-\left(\boldsymbol{A}_1\boldsymbol{W} + \boldsymbol{W}^T\boldsymbol{A}_1\right) \otimes \boldsymbol{I}_b\right)\hat{\boldsymbol{q}} + 2\hat{\boldsymbol{q}}^T\left(\boldsymbol{A}_1 \otimes \boldsymbol{I}_b\right)\dot{\boldsymbol{\psi}} \\ =& \hat{\boldsymbol{q}}^T\left(\boldsymbol{B}_1 \otimes \boldsymbol{I}_b\right)\hat{\boldsymbol{q}} + 2\hat{\boldsymbol{q}}^T\boldsymbol{C}_1 \\ \le& \|\hat{\boldsymbol{q}}\|\left(\lambda_{\max}(\boldsymbol{B}_1)\|\hat{\boldsymbol{q}}\| + 2\|\boldsymbol{C}_1\|\right),\end{aligned} \tag{3.27}$$

where $\boldsymbol{B}_1 = -\boldsymbol{A}_1\boldsymbol{W} - \boldsymbol{W}^T\boldsymbol{A}_1$ and $\boldsymbol{C}_1 = \left(\boldsymbol{A}_1 \otimes \boldsymbol{I}_b\right)\dot{\boldsymbol{\psi}}$. From Lemma 1, it follows that $\boldsymbol{B}_1$ is a negative definite matrix, which implies that $\lambda_{\max}\left(\boldsymbol{B}_1\right) < 0$. Moreover, since $\lim_{t\to\infty} \dot{\boldsymbol{\psi}} = \mathbf{0}_{Pb}$, it gets $\lim_{t\to\infty} \boldsymbol{C}_1 = \mathbf{0}_{Pb}$. This implies that, for any small constant $n_1 > 0$, there exists a finite time $\bar{T}_1 > 0$ such that for all $t \ge \bar{T}_1$, it holds that $\|\boldsymbol{C}_1\| < n_1$. Then, the following inequality holds

$$\dot{\bar{V}}_1 \le \|\hat{\boldsymbol{q}}\|\left(\lambda_{\max}(\boldsymbol{B}_1)\|\hat{\boldsymbol{q}}\| + 2n_1\right), \forall t \ge \bar{T}_1. \tag{3.28}$$

By selecting $\alpha = \frac{o_1 n_1}{-\lambda_{\max}(\boldsymbol{B}_1)} > 0$ with a constant $o_1 > 2$, and noting that Eqs (3.26) and (3.28) satisfy the two conditions required in Lemma 2, it follows that there exists a finite time $\bar{T} \ge \bar{T}_1 > 0$ such that the solution of Eq (3.24) satisfies the following equation:

$$\|\hat{\boldsymbol{q}}\| \le \kappa_1^{-1}\left(\kappa_2\left(\alpha\right)\right) = \sqrt{\frac{\lambda_{\max}(\boldsymbol{A}_1)}{\lambda_{\min}(\boldsymbol{A}_1)}}\alpha = \frac{o_1}{-\lambda_{\max}(\boldsymbol{B}_1)}\sqrt{\frac{\lambda_{\max}(\boldsymbol{A}_1)}{\lambda_{\min}(\boldsymbol{A}_1)}}n_1, \forall t \ge \bar{T}, \tag{3.29}$$

where $\kappa_1(\alpha) = \lambda_{\min}(\boldsymbol{A}_1)\, o_1^2$ and $\kappa_2(\alpha) = \lambda_{\max}(\boldsymbol{A}_1)\, o_1^2$. Since n_1 is an arbitrarily small constant, it follows from Eq (3.29) that, for any given $\bar{\varsigma} > 0$, there exists a finite time $\bar{T} > 0$ such that for all $t \geq \bar{T}$, the inequality $|\hat{\boldsymbol{q}}| \leq \bar{\varsigma}$ holds. Consequently, it gets $\lim_{t\to\infty} \hat{\boldsymbol{q}} = \boldsymbol{0}_{Pb}$, which implies that

$$\lim_{t\to\infty} \left\| \boldsymbol{q}_i(t) - \boldsymbol{q}_d(t) \right\| = 0, \quad \lim_{t\to\infty} \|\dot{\boldsymbol{q}}_i(t) - \dot{\boldsymbol{q}}_d(t)\| = 0.$$

□

Remark 4. *Theorem 1 establishes the tracking control strategy for NUELSs by formulating an energy-shaping design within the passivity-based framework. Distinct from existing consensus approaches for NUELSs [8, 30–32], the proposed method reconstructs the potential and kinetic energy of the interconnected system, the energy of the adaptive updating law and incorporates damping injection to guarantee stability. This formulation not only enhances the analytical tractability but also provides a new perspective for the control of NUELSs.*

3.2. Passivity-based tracking control with communication delays

The previous subsection designed and analyzed a passivity-based tracking controller for the case without communication delays, verifying its effectiveness in ensuring system stability. The following subsection extends the study to the controller design and stability analysis in the presence of communication delays.

To achieve this, the passivity-based control input for NUELSs is presented as

$$\bar{\boldsymbol{\tau}}_i = \boldsymbol{F}_i(\boldsymbol{x}_i - \boldsymbol{q}_i) + \boldsymbol{U}_i \ddot{\bar{\boldsymbol{r}}}_i - \boldsymbol{F}_i\left(\bar{\boldsymbol{e}}_i - \bar{\boldsymbol{\psi}}_i\right) - \boldsymbol{Q}_i(\bar{\boldsymbol{e}}_i - \boldsymbol{\varepsilon}_i), \tag{3.30}$$

here the reference position with communication delays

$$\dot{\bar{\boldsymbol{s}}}_i = -k\sum_{j=1}^{P} a_{ij}\left(\hat{\boldsymbol{q}}_i - \hat{\boldsymbol{q}}_j(t-T)\right) - k\beta_i\hat{\boldsymbol{q}}_i + \dot{\boldsymbol{q}}_d, \tag{3.31}$$

where T stands for the communication delay, the sliding vector

$$\dot{\bar{\boldsymbol{\psi}}}_i = \dot{\boldsymbol{q}}_i - \dot{\bar{\boldsymbol{s}}}_i, \tag{3.32}$$

two intermediate variables

$$\bar{\boldsymbol{e}}_i = \boldsymbol{x}_i - \bar{\boldsymbol{r}}_i, \tag{3.33}$$

and

$$\bar{\boldsymbol{r}}_i = \boldsymbol{q}_i + \boldsymbol{F}_i^{-1}\bar{\boldsymbol{Y}}_i\check{\boldsymbol{\chi}}_i - \bar{\boldsymbol{\psi}}_i, \tag{3.34}$$

the corresponding updating law

$$\dot{\check{\boldsymbol{\chi}}}_i = -\bar{\boldsymbol{\delta}}_i\bar{\boldsymbol{Y}}_i^T(\boldsymbol{q}_i, \dot{\boldsymbol{q}}_i, \dot{\bar{\boldsymbol{s}}}_i, \ddot{\bar{\boldsymbol{s}}}_i)\dot{\bar{\boldsymbol{\psi}}}_i, \tag{3.35}$$

where $\check{\boldsymbol{\chi}}_i$ denotes the estimate of $\boldsymbol{\chi}_i$, $\bar{\boldsymbol{\delta}}_i$ stands for a symmetric and positive definite matrix.

To summarize, the closed-loop system is described by the following equation

$$\begin{aligned} &\boldsymbol{M}_i(\boldsymbol{q}_i)\ddot{\bar{\boldsymbol{\psi}}}_i + \boldsymbol{C}_i(\boldsymbol{q}_i, \dot{\boldsymbol{q}}_i)\dot{\bar{\boldsymbol{\psi}}}_i + \bar{\boldsymbol{Y}}_i\hat{\boldsymbol{\chi}}_i + \boldsymbol{F}_i\left(\bar{\boldsymbol{\psi}}_i - \bar{\boldsymbol{e}}_i\right) = \boldsymbol{0}_b; \\ &\boldsymbol{U}_i\ddot{\bar{\boldsymbol{e}}}_i + \boldsymbol{F}_i\left(\bar{\boldsymbol{e}}_i - \bar{\boldsymbol{\psi}}_i\right) = -\boldsymbol{Q}_i(\bar{\boldsymbol{e}}_i - \boldsymbol{\varepsilon}_i), \end{aligned} \tag{3.36}$$

where the estimated error $\hat{\boldsymbol{\chi}}_i = \boldsymbol{\chi}_i - \check{\boldsymbol{\chi}}_i$.

Theorem 2. *For the NUELSs (2.1) under Assumptions 1 and 2, the proposed passivity-based control protocol (3.30) in the presence of communication delays, together with the updating law (3.35) can solve the tracking problem in the sense of Definition 1.*

Proof. Consider the total energy of the closed-loop system defined by the Lyapunov function $V_2 = {}^s\bar{I} + {}^c\bar{I} + {}^r\bar{I}$. Similarly, the derivative of V_2 with respect to time is given by $\dot{V}_2 = -\dot{\boldsymbol{\varepsilon}}^T \boldsymbol{H}\dot{\boldsymbol{\varepsilon}} \leq 0$.

The proof of Theorem 2 is similar to that of Theorem 1 and thus omitted for brevity, from which it follows that $\lim_{t\to\infty} \dot{\bar{\boldsymbol{\psi}}}_i = \mathbf{0}_b$.

By applying the Laplace transform to Eqs (3.31) and (3.32), it follows that

$$l\boldsymbol{\Gamma}_i(l) - \hat{\boldsymbol{q}}_i(0) = -k\sum_{j=1}^{P} a_{ij}[\boldsymbol{\Gamma}_i(l) - e^{-Tl}\boldsymbol{\Gamma}_j(l)] - k\beta_i\boldsymbol{\Gamma}_i(l) + \boldsymbol{\Psi}_i(l) - \bar{\boldsymbol{\psi}}_i(0), \tag{3.37}$$

where $\boldsymbol{\Gamma}_i(l)$ and $\boldsymbol{\Psi}_i(l)$ are the Laplace transforms of $\hat{\boldsymbol{q}}_i$ and $\bar{\boldsymbol{\psi}}_i$, respectively. Accordingly, Eq (3.37) can be reformulated in the vector form

$$l\boldsymbol{\Gamma}(l) = -\left[\left(\bar{\boldsymbol{D}} - \bar{\boldsymbol{Z}} + \bar{\boldsymbol{\sigma}}\right) \otimes \boldsymbol{I}_b\right]\boldsymbol{\Gamma}(l) + \hat{\boldsymbol{q}}(0) + \boldsymbol{\Psi}(l) - \bar{\boldsymbol{\psi}}(0), \tag{3.38}$$

where

$$\bar{\boldsymbol{D}}=diag[\sum_{j=1}^{P} ka_{ij}],\quad \bar{\boldsymbol{Z}}=\text{diag}[ka_{ij}e^{-Tl}],\quad \bar{\boldsymbol{\sigma}} = diag\left[k\beta_1, \cdots k\beta_N\right],$$

$\boldsymbol{\Gamma}(l)$, $\boldsymbol{\Psi}(l)$, $\hat{\boldsymbol{q}}(0)$ and $\bar{\boldsymbol{\psi}}(0)$ are the column vectors of $\boldsymbol{\Gamma}_i(l)$, $\boldsymbol{\Psi}_i(l)$, $\hat{\boldsymbol{q}}_i(0)$ and $\bar{\boldsymbol{\psi}}_i(0)$.

Then Eq (3.38) can be reformulated as

$$\boldsymbol{\Gamma}(l) = [\boldsymbol{\Phi}(l) \otimes \boldsymbol{I}_b]\left[\hat{\boldsymbol{q}}(0) + \boldsymbol{\Psi}(l) - \bar{\boldsymbol{\psi}}(0)\right], \tag{3.39}$$

where

$$\boldsymbol{\Phi}(l) = [b\boldsymbol{I}_P + \bar{\boldsymbol{D}} - \bar{\boldsymbol{Z}} + \bar{\boldsymbol{\sigma}}]^{-1}.$$

Equation (3.39) is transformed into the following expression for $\dot{\hat{\boldsymbol{q}}}$

$$\boldsymbol{\Gamma}_v(l) = l\boldsymbol{\Gamma}(l) - \hat{\boldsymbol{q}}(0) = [\boldsymbol{\Phi}(l) \otimes \boldsymbol{I}_b][l\hat{\boldsymbol{q}}(0) + l\boldsymbol{\Psi}(l) - l\bar{\boldsymbol{\psi}}(0)] - \hat{\boldsymbol{q}}(0). \tag{3.40}$$

Applying Gershgorin theorem, it can be concluded that the matrix $\boldsymbol{\Phi}(l)$ is free of poles in the open half-plane, thereby ensuring $\boldsymbol{\Phi}^{-1}(0)$ is non-zero.

Therefore, by applying the final value theorem, the following result is obtained

$$\begin{aligned}\lim_{t\to\infty} \dot{\hat{\boldsymbol{q}}} &= \lim_{l\to 0} l\boldsymbol{\Gamma}_v(l)\\ &= [\boldsymbol{\Phi}(0) \otimes \boldsymbol{I}_b][\lim_{l\to 0} l^2\hat{\boldsymbol{q}}(0) + \lim_{l\to 0} l^2\boldsymbol{\Psi}(l)\\ &\quad - \lim_{l\to 0} l^2\bar{\boldsymbol{\psi}}(0)] - \lim_{l\to 0} l\hat{\boldsymbol{q}}(0)\\ &= \mathbf{0}_{Pb}.\end{aligned} \tag{3.41}$$

From Eq (3.41), it has $\dot{\boldsymbol{q}} \to \dot{\boldsymbol{q}}_d$ as $t \to \infty$. Meanwhile, since $\bar{\boldsymbol{\psi}} \to 0_{Pb}$ as $t \to \infty$, the following equation is satisfied

$$\begin{aligned}\lim_{t\to\infty} \hat{\boldsymbol{q}} &= \lim_{l\to 0} l\boldsymbol{\Gamma}(l) \\ &= [\boldsymbol{\Phi}(0) \otimes \boldsymbol{I}_b] [\lim_{l\to 0} l\hat{\boldsymbol{q}}(0) + \lim_{l\to 0} l\boldsymbol{\Psi}(l) - \lim_{l\to 0} l\bar{\boldsymbol{\psi}}(0)] \\ &= \mathbf{0}_{Pb}.\end{aligned} \tag{3.42}$$

Eventually, by combining Eqs (3.31), (3.32), (3.41), and (3.42), it follows that

$$\lim_{t\to\infty} \hat{\boldsymbol{q}}_i = \mathbf{0}_b, \quad \lim_{t\to\infty} \dot{\hat{\boldsymbol{q}}}_i = \mathbf{0}_b.$$

Consequently, $\lim_{t\to\infty} (\hat{\boldsymbol{q}}_i - \hat{\boldsymbol{q}}_j(t-T)) = \mathbf{0}_b$, and with $\hat{\boldsymbol{q}}_j(t-T) = \hat{\boldsymbol{q}}_j(t) - \int_{t-T}^{t} \dot{\hat{\boldsymbol{q}}}_j(\varpi - T)d\varpi$, this is equivalent to $\hat{\boldsymbol{q}}_i \to \hat{\boldsymbol{q}}_j$ as $t \to \infty$. Therefore,

$$\lim_{t\to\infty} \|\boldsymbol{q}_i(t) - \boldsymbol{q}_d(t)\| = 0, \quad \lim_{t\to\infty} \left\|\dot{\boldsymbol{q}}_i(t) - \dot{\boldsymbol{q}}_d(t)\right\| = 0,$$

which completes the proof of Theorem 2.

□

Remark 5. *The communication delay considered in this work originates from the networked exchange of information among agents and acts only on the information or control channel. The intrinsic dynamics of NUELSs are inherently delay free [8, 17, 34]. As a result, the delay affects only the timing of the control law updates and does not change the mathematical structure of NUELSs.*

Remark 6. *Building upon Theorem 1, Theorem 2 generalizes the suggested passivity-based framework to scenarios with communication delays, achieving effective tracking control of NUELSs via the energy-shaping approach. Unlike conventional energy-shaping strategies [20–22], this method accounts for underactuated characteristics while incorporating sliding mode variables, adaptive updating law, and damping injection. The resulting control scheme ensures closed-loop stability and improved tracking performance, offering practical application value in practical multi-agent engineering systems.*

4. Numerical simulations

To further substantiate the theoretical results, this section conducts numerical simulations under both scenarios with and without communication delays. Specifically, a flexible-joint manipulator with two links, governed by underactuated EL dynamics and depicted in Figure 1, is employed as the representative test system. Its dynamics can be formulated in the standard form of system (2.1), expressed as follows:

$$\boldsymbol{M}_i(\boldsymbol{q}_i) = \begin{bmatrix} \theta_i + 2\varsigma_i \cos q_{i_2} & z_i + \varsigma_i \cos q_{i_2} \\ z_i + \varsigma_i \cos q_{i_2} & z_i \end{bmatrix},$$

$$\boldsymbol{C}_i(\boldsymbol{q}_i, \dot{\boldsymbol{q}}_i) = \begin{bmatrix} -\varsigma_i \dot{q}_{i_2} \sin q_{i_2} & -\varsigma_i (\dot{q}_{i_1} + \dot{q}_{i_2}) \sin q_{i_2} \\ \varsigma_i \dot{q}_{i_1} \sin q_{i_2} & 0 \end{bmatrix},$$

$$\boldsymbol{G}_i(\boldsymbol{q}_i) = \begin{bmatrix} g\varphi_{i_1}(\xi_{i_1} + \xi_{i_2})\cos q_{i_1} + g\varphi_{i_2}\cos(q_{i_1} + q_{i_2}) \\ g\varphi_{i_2}\cos(q_{i_1} + q_{i_2}) \end{bmatrix},$$

$\theta_i = \varphi_{i_2}^2\xi_{i_2} + \varphi_{i_1}^2(\xi_{i_1} + \xi_{i_2})$, $\varsigma_i = \varphi_{i_1}\varphi_{i_2}\xi_{i_2}$, $z_i = \varphi_{i_2}^2\xi_{i_2}$, P= 5 and $b = 2$, where ξ_i denotes the mass of each link, φ_i represents the corresponding link length, and $g = 9.81m/s^2$ is the gravitational acceleration. The detailed parameter values are provided in Table 1, from which the regression matrix is subsequently formulated as:

$$\boldsymbol{Y}_i = \begin{bmatrix} \ddot{s}_{i_1} & Y_{12} & \ddot{s}_{i_2} & g\cos q_{i_1} & g\cos(q_{i_1} + q_{i_2}) \\ 0 & Y_{21} & \ddot{s}_{i_1} + \ddot{s}_{i_2} & 0 & g\cos(q_{i_1} + q_{i_2}) \end{bmatrix},$$

where the parameter vector

$$\boldsymbol{\eta}_i = [\theta_i, \varsigma_i, z_i, \varphi_{i_1}(\xi_{i_1} + \xi_{i_2}), \varphi_{i_2}\xi_{i_2}]^T,$$

$$Y_{12} = 2\ddot{s}_{i_1}\cos q_{i_2} + \ddot{s}_{i_2}\cos q_{i_2} - \dot{s}_{i_1}\dot{q}_{i_2}\sin q_{i_2} - (\dot{q}_{i_1} + \dot{q}_{i_2})\dot{s}_{i_2}\sin q_{i_2},$$

$$Y_{21} = \ddot{s}_{i_1}\cos q_{i_2} + \dot{s}_{i_1}\dot{q}_{i_1}\sin q_{i_2}.$$

To validate the general applicability of the proposed approach, the initial states of the NUELSs, including positions and velocities, are initialized arbitrarily. Numerical simulations under these conditions confirm the robustness and tracking performance of the passivity-based energy-shaping control framework.

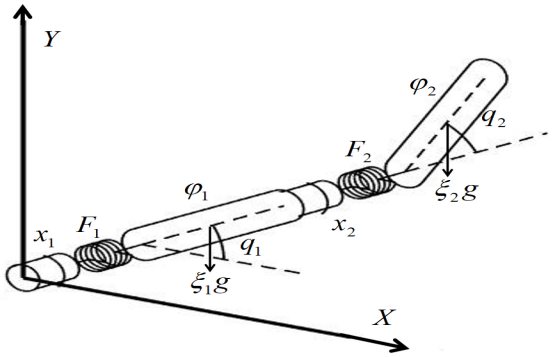

Figure 1. Modeling schematic of the two-link underactuated EL system.

Table 1. Model parameters of NUELSs.

Parameters	System 1	System 2	System 3	System 4	System 5
$\xi_1(kg)$	3.5	4.3	5.6	4.1	3.6
$\xi_2(kg)$	4.1	5.8	3.2	5.4	4.2
$\varphi_1(m)$	0.8	1.2	0.5	1.7	1.2
$\varphi_2(m)$	1.8	1.7	0.4	1.0	0.8
$\boldsymbol{F}_i$	$43\boldsymbol{I}_2$	$43\boldsymbol{I}_2$	$43\boldsymbol{I}_2$	$43\boldsymbol{I}_2$	$43\boldsymbol{I}_2$
$\boldsymbol{U}_i$	$diag(0.8, 1.1)$	$diag(1.4, 1.3)$	$diag(1.2, 1.8)$	$diag(0.5, 1.0)$	$diag(0.6, 0.9)$

4.1. NUELSs without communication delays

For validation purposes, the communication topology presented in Figure 2 is considered to evaluate the numerical performance of the passivity-based energy-shaping tracking control framework for NUELSs. Specifically, nodes 1–5 represent five underactuated systems, whereas node 0 as a virtual leader transmitting reference signals to systems 1 and 5. The initial value of $\check{\boldsymbol{\eta}}_i$ is selected to be zero, $\boldsymbol{q}_d(t) = [0.5\cos t, 0.5\sin t]^T$, $\boldsymbol{\delta}_i = \boldsymbol{I}_5$, $k = 1$, $\boldsymbol{h}_i = 27$, and $\boldsymbol{Q}_i = 13\boldsymbol{I}_2$, which is in accordance with the conditions specified in Theorem 1. Based on the aforementioned conditions, numerical simulations yield the results summarized in Figure 3. As shown in Figure 3(a), the angular position of the link evolves over 0–10 s, while Figure 3(b) depicts the associated tracking error relative to the desired reference. The velocity of link angular is reported in Figure 3(c), and its deviation from the desired velocity is presented in Figure 3(d). The results clearly demonstrate that, without communication delays, the NUELSs converge asymptotically to the desired trajectory q_d. This verifies the effectiveness of the proposed passivity-based energy-shaping strategy, where the integration of control input (3.10) and adaptive updating law (3.9) ensures successful realization of the tracking control objective.

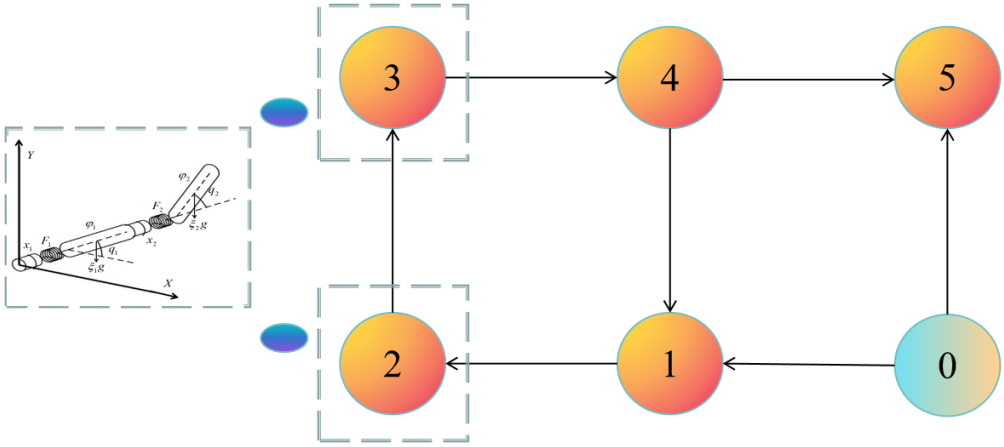

Figure 2. Communication topology $\mathcal{D}$.

4.2. NUELSs with communication delays

This subsection also employs Figure 2 as the communication topology. With the initial value of $\check{\boldsymbol{\chi}}_i$ is chosen to zero and the parameters specified as $\bar{\boldsymbol{\delta}}_i = \boldsymbol{I}_5$ and $T = 0.02$, the setup is in full compliance with the conditions of Theorem 2. The remaining parameters follow the same selections as in the scenario without communication delays. Based on these settings, numerical simulations are performed, and the corresponding results are shown in Figure 4. The link angular position trajectory and its tracking error with respect to the desired reference are presented in Figure 4(a),4(b). Likewise, Figure 4(c),4(d) shows the velocity of link angular and the corresponding tracking error. To better illustrate how variations in communication delay affect the closed-loop cooperative tracking performance, Figure 5(a),5(b) depicts the position and velocity responses of the first link under communication delays of $T = 0.1$

and $T = 1$, respectively. As observed from Figures 3–5, increasing the communication delay leads to a longer convergence time of the NUELSs, while the cooperative tracking objective remains achieved. Accordingly, by employing the control protocol (3.30) in conjunction with the adaptive updating law (3.35), the passivity-based energy-shaping tracking control strategy in the presence of communication delays for NUELSs is effectively established.

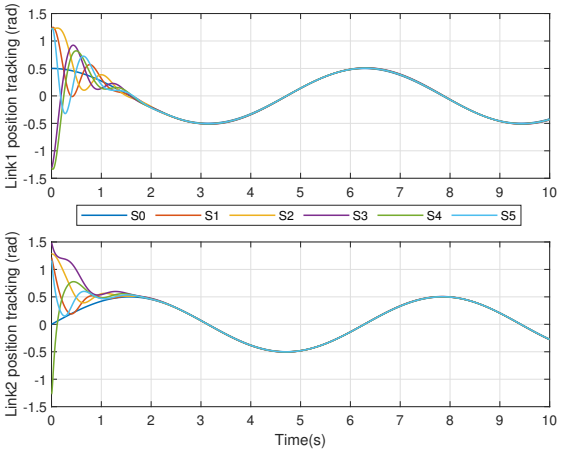

(a) The angular position of the link $\boldsymbol{q}_i$.

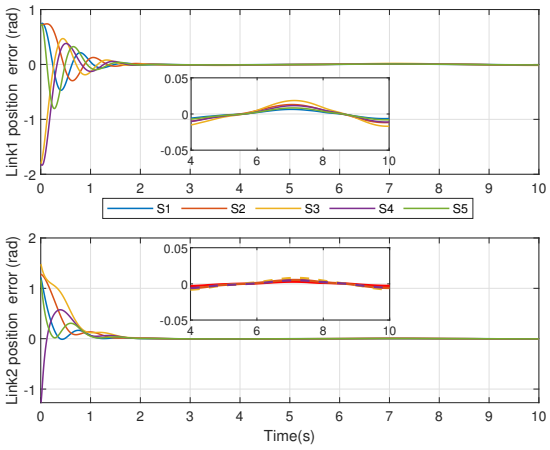

(b) The error of link angular position.

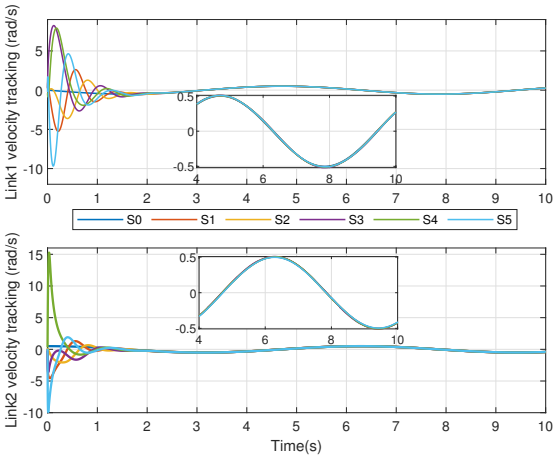

(c) The velocity of link angular position $\dot{\boldsymbol{q}}_i$.

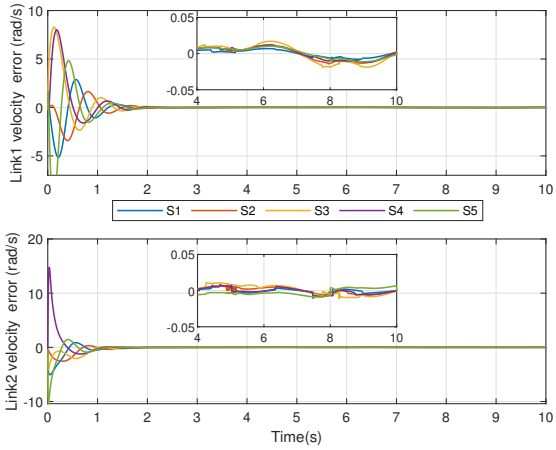

(d) The velocity error of link angular position.

Figure 3. NUELSs without communication delays.

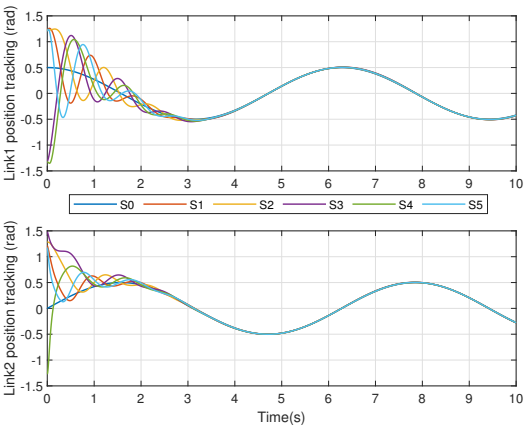

(a) The angular position of the link $\boldsymbol{q}_i$.

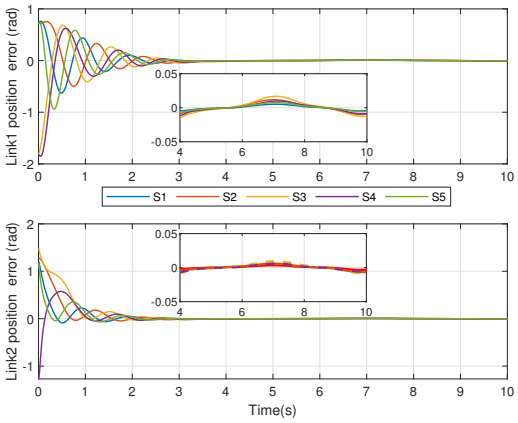

(b) The error of link angular position.

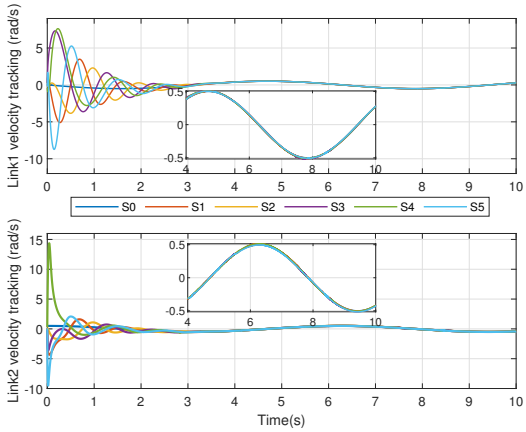

(c) The velocity of link angular position $\dot{\boldsymbol{q}}_i$.

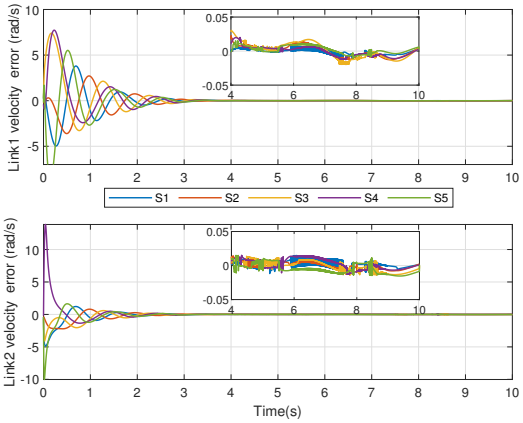

(d) The velocity error of link angular position.

Figure 4. Communication delays $T = 0.02$.

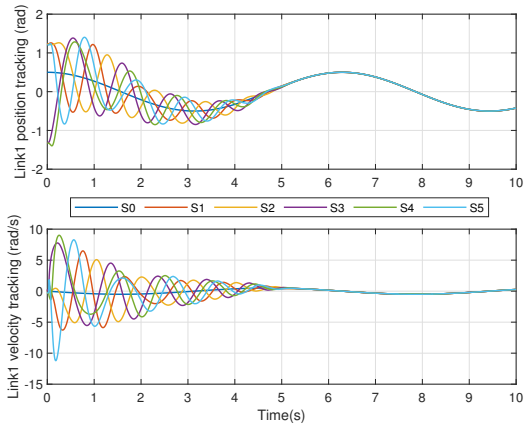

(a) communication delays $T = 0.1$.

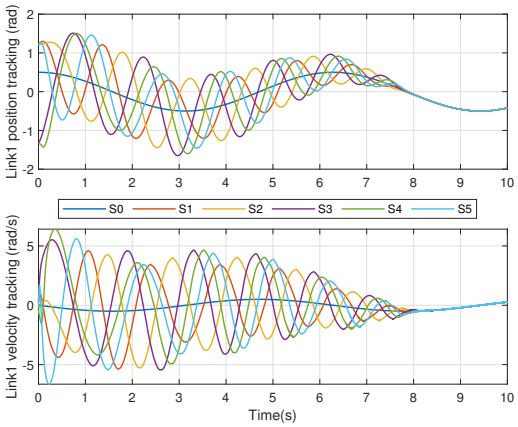

(b) communication delays $T = 1$.

Figure 5. The angular position and velocity of the first link.

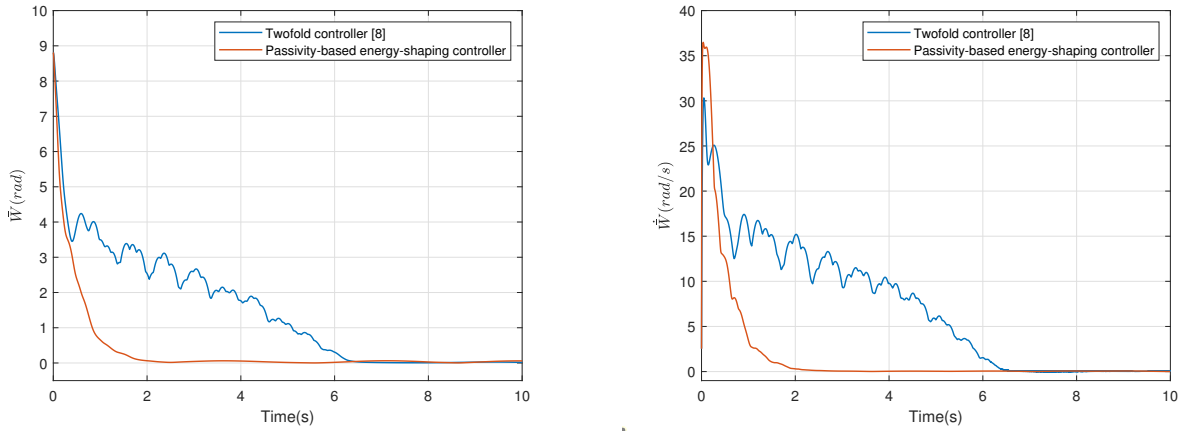

Figure 6. Evolution of $\bar{W}$ and $\dot{\bar{W}}$.

4.3. Comparative performance analysis

As noted earlier, the proposed tracking control approach for NUELSs leverages energy-shaping within a passivity-based control framework, providing stronger robustness and adaptability to underactuated constraints than conventional methods [6–8, 29–33]. To more intuitively illustrate the performance advantages of the proposed strategy over existing controllers, two indices are introduced to evaluate the overall cooperative tracking performance under different control algorithms, as shown below:

$$\bar{W} = \sum_{i=1}^{5} \left\| \boldsymbol{q}_i - \boldsymbol{q}_d \right\| = \sum_{i=1}^{5} \sqrt{(q_{i_1} - q_{d_1})^2 + (q_{i_2} - q_{d_2})^2}, \tag{4.1}$$

and

$$\dot{\bar{W}} = \sum_{i=1}^{5} \left\| \dot{\boldsymbol{q}}_i - \dot{\boldsymbol{q}}_d \right\| = \sum_{i=1}^{5} \sqrt{(\dot{q}_{i_1} - \dot{q}_{d_1})^2 + (\dot{q}_{i_2} - \dot{q}_{d_2})^2}. \tag{4.2}$$

Comparison with the twofold controller (3) reported in [8] is carried out to further examine the performance of the proposed control strategy. In order to reduce the influence of additional variables, both controllers are tested under identical initial conditions, communication topology, and system parameters, the desired position is specified as $\boldsymbol{q}_d = [-3, 2]^T$, and the communication delay is fixed at $T = 0.02$ in the numerical simulations. Results presented in Figure 6 indicate that the passivity-based energy-shaping controller exhibits smoother transient behavior and faster convergence with respect to both performance metrics when compared with the twofold controller. Moreover, the proposed approach is capable of tracking time-varying reference trajectories, thereby extending its applicability beyond fixed point tracking.

5. Conclusions

This paper has presented two passivity-based energy-shaping tracking control schemes for NUELSs. By integrating adaptive control techniques and sliding mode variables into the passivity-based control framework, the proposed strategies ensure closed-loop stability, asymptotic tracking, and robustness against communication delays. Comprehensive numerical simulations on NUELSs

confirmed the theoretical findings, showing that the suggested passivity-based controllers achieve reliable tracking performance in the presence and absence of communication delays. The results further reveal that communication delays mainly influence the transient response, while the overall stability and convergence properties remain preserved.

Several extensions of this work will be considered in our future research. Although a common reference trajectory is adopted to focus on cooperative tracking under network constraints, the proposed passivity-based energy-shaping framework may be extended to agent specific reference trajectories through a suitable redefinition of tracking errors. Furthermore, incorporating prescribed performance constraints into the present framework constitutes a promising research direction, since such results for NUELSs remain largely unexplored. In addition, extensions to more general network conditions, such as time-varying communication delays and switching interaction topology, are also of interest.

Author contributions

Bin Zheng: Conceptualization, Data curation, Formal analysis, Methodology, Funding acquisition, Project administration, Validation, Visualization, Writing-review & editing. Runlong Peng: Data curation, Formal analysis, Investigation, Software, Visualization. Xuewei Ling: Resources, Funding acquisition, Project administration, Supervision, Writing-review & editing. All authors have read and approved the final version of the manuscript for publication.

Use of Generative-AI tools declaration

The authors declare they have not used Artificial Intelligence (AI) tools in the creation of this article.

Acknowledgments

The authors would like to express their gratitude to the editor and anonymous reviewers for their insightful and constructive comments, which enhanced the quality of this paper. This work was supported by the Foundation for Cultivated Young Talents of Fujian Province, China (No.2025350266), and by the Natural Science Basic Research Program of Shaanxi Province (No.2024JC-YBQN-0025).

Conflict of interest

The authors declare no competing interests.

References

1. T. Li, J. Zhang, S. Li, P. Zhou, D. Lv, Neural-based adaptive fixed-time prescribed performance control for the flexible-joint robot with actuator failures, *Nonlinear Dyn.*, **111** (2023), 16187–16214. https://doi.org/10.1007/s11071-023-08714-1
2. H. Zhong, W. Wen, J. Fan, W. Yang, Reinforcement learning-based adaptive tracking control for flexible-joint robotic manipulators, *AIMS Math.*, **9** (2024), 27330–27360. https://doi.org/10.3934/math.20241328

3. W. Sun, S. Su, J. Xia, V. Nguyen, Adaptive fuzzy tracking control of flexible-joint robots with full-state constraints, *IEEE Trans. Syst. Man Cybern. Syst.*, **49** (2018), 2201–2209. http://doi.org/10.1109/TSMC.2018.2870642
4. G. Chen, Y. Xu, X. Yang, H. Hu, H. Cheng, L. Zhu, et al., Target tracking control of a bionic mantis shrimp robot with closed-loop central pattern generators, *Ocean Eng.*, **297** (2024), 116963. http://doi.org/10.1016/j.oceaneng.2024.116963
5. Y. Xiao, Y. Yang, D. Ye, Y. Zhao, Scaling-transformation-based attitude tracking control for rigid spacecraft with prescribed time and prescribed bound, *IEEE Trans. Aerosp. Electron. Syst.*, **61** (2025), 433–442. http://doi.org/10.1109/TAES.2024.3451454
6. H. Bilal, B. Yin, M. Aslam, Z. Anjum, A. Rohra, Y. Wang, A practical study of active disturbance rejection control for rotary flexible joint robot manipulator, *Soft Comput.*, **27** (2023), 4987–5001. http://doi.org/10.1007/s00500-023-08026-x
7. H. Ma, Q. Zhou, H. Li, R. Lu, Adaptive prescribed performance control of a flexible-joint robotic manipulator with dynamic uncertainties, *IEEE Trans. Cybern.*, **52** (2022), 12905–12915. http://doi.org/10.1109/TCYB.2021.3091531
8. E. Nuño, D. Valle, I. Sarras, L. Basañez, Leader–follower and leaderless consensus in networks of flexible-joint manipulators, *Eur. J. Control*, **20** (2014), 249–258. https://doi.org/10.1016/j.ejcon.2014.07.003
9. C. Wang, J. Wang, R. Agarwal, Z. Li, Almost anti-periodic discrete oscillation of general N-dimensional mechanical system and underactuated Euler-Lagrange system, *Appl. Sci.*, **12** (2022), 1991. https://doi.org/10.3390/app12041991
10. T. Sun, X. Zhang, H. Yang, Y. Pan, Singular perturbation-based saturated adaptive control for underactuated Euler-Lagrange systems, *ISA Trans.*, **119** (2022), 74–80. https://doi.org/10.1016/j.isatra.2021.02.036
11. B. Zheng, J. Ji, R. Peng, Z. Miao, J. Zhou, Energy shaping-based consensus control in networked underactuated Euler-Lagrange systems with communication and input delays, *J. Franklin Inst.*, **361** (2024), 106705. https://doi.org/10.1016/j.jfranklin.2024.106705
12. J. Romero, B. Yi, Immersion and invariance orbital stabilization of underactuated mechanical systems with collocated pre-feedback, *J. Robust Nonlinear Control*, **34** (2024), 9421–9437. https://doi.org/10.1002/rnc.7467
13. M. Mattioni, P. Borja, Digital passivity-based control of underactuated mechanical systems, *Automatica*, **173** (2025), 112096. https://doi.org/10.1016/j.automatica.2024.112096
14. J. Acosta, R. Ortega, A. Astolfi, A. Mahindrakar, Interconnection and damping assignment passivity-based control of mechanical systems with underactuation degree one, *IEEE Trans. Autom. Control*, **50** (2005), 1936–1955. https://doi.org/10.1109/TAC.2005.860292
15. K. Hamada, P. Borja, J. Scherpen, K. Fujimoto, I. Maruta, Passivity-based lag-compensators with input saturation for mechanical port-Hamiltonian systems without velocity measurements, *IEEE Control Syst. Lett.*, **5** (2021), 1285–1290. https://doi.org/10.1109/LCSYS.2020.3032890
16. N. Sakata, K. Fujimoto, I. Maruta, Passivity-based sliding mode control for mechanical port-Hamiltonian systems, *IEEE Trans. Autom. Control*, **69** (2024), 5605–5612. https://doi.org/10.1109/TAC.2024.3371898

17. E. Nuño, R. Ortega, Achieving consensus of Euler-Lagrange agents with interconnecting delays and without velocity measurements via passivity-based control, *IEEE Trans. Control Syst. Technol.*, **26** (2018), 222–232. http://doi.org/10.1109/TCST.2017.2661822
18. E. Cruz-Zavala, E. Nuño, J. Moreno, Finite-time consensus of Euler-Lagrange agents without velocity measurements via energy shaping, *J. Robust Nonlinear Control*, **29** (2019), 6006–6030. http://doi.org/10.1002/rnc.4704
19. B. Zheng, J. Ji, R. Peng, Z. Miao, J. Zhou, Region-reaching control for multiple underactuated Euler-Lagrange systems based on energy-shaping framework, *Commun. Nonlinear Sci. Numer. Simul.*, **151** (2025), 109020. https://doi.org/10.1016/j.cnsns.2025.109020
20. M. Galaz, R. Ortega, A. Bazanella, A. Stankovic, An energy-shaping approach to the design of excitation control of synchronous generators, *Automatica*, **39** (2003), 111–119. https://doi.org/10.1016/S0005-1098(02)00177-2
21. J. Sandoval, R. Kelly, V. Santibáñez, J. Moreno-Valenzuela, L. Cervantes-Pérez, Partial potential energy shaping control of torque-driven robot manipulators in joint space, *Int. J. Control Autom. Syst.*, **22** (2024), 2230–22419. http://doi.org/10.1007/s12555-022-1196-z
22. B. Salamat, G. Elsbacher, A. Tonello, Energy shaping control in underactuated robot systems with underactuation degree two, *IEEE Robot. Autom. Lett.*, **10** (2025), 2734–2741. http://doi.org/10.1109/LRA.2025.3534688
23. J. Sun, Y. Dang, S. Yang, J. Wang, Y. Cai, A grey incidence model with cumulative time-delay effects and its applications, *Appl. Math. Model.*, **145** (2025), 116144. http://doi.org/10.1016/j.apm.2025.116144
24. Y. Zhao, H. Wu, Fixed/Prescribed stability criterions of stochastic system with time-delay, *AIMS Math.*, **9** (2024), 14425–14453. http://doi.org/10.3934/math.2024701
25. H. Zeng, Y. Chen, Y. He, X. Zhang, A delay-derivative-dependent switched system model method for stability analysis of linear systems with time-varying delay, *Automatica*, **175** (2025), 112183. http://doi.org/10.1016/j.automatica.2025.112183
26. J. Wen, F. Wang, Exponential stabilization of stochastic quantum systems based on time-delay noise-assisted feedback, *Chaos Solit. Fract.*, **186** (2024), 115228. https://doi.org/10.1016/j.chaos.2024.115228
27. J. Zhang, J. Wang, H. Han, Y. Hou, Coevolution-based robust optimal control for nonlinear system with time-delay optimal objectives, *IEEE Trans. Syst. Man Cybern. Syst.*, **55** (2025), 1126–1136. https://doi.org/10.1109/TSMC.2024.3496564
28. D. Li, L. Cao, Y. Pan, W. Xiao, H. Xue, A novel communication time-delay cooperative control method with switching event-triggered strategy, *J. Intell. Robot. Syst.*, **110** (2024), 43. https://doi.org/10.1007/s10846-024-02076-5
29. Y. Fan, Z. Jin, B. Guo, X. Luo, X. Guan, Finite-time consensus of networked Euler-Lagrange systems via STA-based output feedback, *Int. J. Control Autom. Syst.*, **20** (2022), 2993–3005. https://doi.org/10.1007/s12555-021-0393-5
30. R. Peng, R. Guo, L. Liu, J. Ji, Z. Miao, J. Zhou, Practical consensus tracking control for networked Euler–Lagrange systems based on UDE integrated with RBF neural network, *Neurocomputing*, **583** (2024), 127544. http://doi.org/10.1016/j.neucom.2024.127554

31. T. Wang, W. Zou, X. Wang, J. Guo, Z. Xiang, Event-triggered fully distributed asymptotic consensus for leaderless multiple Euler-Lagrange systems, *J. Franklin Inst.*, **360** (2023), 8569–8584. http://doi.org/10.1016/j.jfranklin.2023.06.035
32. S. Wang, H. Zhang, S. Baldi, R. Zhong, Leaderless consensus of heterogeneous multiple Euler-Lagrange systems with unknown disturbance, *IEEE Trans. Autom. Control*, **68** (2023), 2399–2406. http://doi.org/10.1109/TAC.2022.3172594
33. Y. Liu, P. Liu, B. Zhang, Distributed finite-time optimization for networked Euler-Lagrange systems under a directed graph, *Trans. Inst. Meas. Control*, **47** (2025), 381–386. http://doi.org/10.1177/01423312241248250
34. Z. Miao, J. Yu, J. Ji, J. Zhou, Multi-objective region reaching control for a swarm of robots, *Automatica*, **103** (2019), 81–87. http://doi.org/10.1016/j.automatica.2019.01.017
35. Y. Liu, Y. Jia, Adaptive consensus control for multiple Euler-Lagrange systems with external disturbance, *Int. J. Control Autom. Syst.*, **15** (2017), 205–211. http://doi.org/10.1007/s12555-015-0221-x

AIMS Press